International Journal of Mass Spectrometry 286 (2009) 112–121

Contents lists available at ScienceDirect

International Journal of Mass Spectrometry

journal homepage: www.elsevier.com/locate/ijms

Interpretation of the characteristic fragmentation mechanisms through determining the initial ionization site by natural spin density: A study on the derivatives of tryptophan and tryptamine

Yong-Zhong Ouyang[a], Yi-Zeng Liang[a,*], Shuhua Li[b], Xiao Luo[a], Liangxiao Zhang[a], Zhonghai Tang[a,c], Qin Wang[a], Xiaona Xu[a,d]

[a] College of Chemistry and Chemical Engineering, Research Center of Modernization of Chinese Medicines, Central South University, Changsha 410083, People's Republic of China
[b] Department of Chemistry, Institute of Theoretical and Computational Chemistry, Key Laboratory of Mesoscopic Chemistry of MOE, Nanjing University, Nanjing 210093, People's Republic of China
[c] College of Bioscience and Biotechnology, Hunan Agriculture University, Changsha 410128, People's Republic of China
[d] College of Chemistry and Chemical Engineering, University of South China, Hengyang, Hunan 421001, People's Republic of China

ARTICLE INFO

Article history:
Received 13 May 2009
Received in revised form 11 July 2009
Accepted 13 July 2009
Available online 23 July 2009

Keywords:
Characteristic fragmentation mechanism
Initial ionization site
Radical site
Atomic spin density
Ionization energy

ABSTRACT

The characteristic fragmentation mechanisms of the derivatives of tryptophan and tryptamine are investigated by the density functional theory (DFT) at the B3LYP/6–31+G (d, p) level. The main primary α-cleavage fragmentation has been predicted through determining the initial ionization site by calculated spin density of molecular radical cation and the variation of molecular structures from neutral to cationic form. The results show that the more intensive base peak produced by main primary α-cleavage fragmentation predicted in the present agrees well with those of experimental mass spectra, which is useful for characterizing the fragmentation mechanisms of such indole alkaloids. More importantly, the novel method for determining the most likely initial ionization site proposed in this study is prior to that based on the ionization energy (IE). It will play an important role in unraveling the mechanisms of radical-driven fragmentation not only for small molecules, but also for gas-phase peptides occurring in electron capture dissociation (ECD), electron transfer dissociation (ETD), or low-energy CID of peptide radical cations. However, this study is inappropriate for negative systems.

1. Introduction

In recent years, mass spectrometry has played an increasingly important role in the identification of molecules of biological interest [1,2]. Until now, electron ionization source (EI) mass spectrometry is still the most common ionization method of choice for many laboratories that routinely analyze volatilizable low molecular mass compounds such as drugs, herbal medicines, flavor and odor components, pesticides, and petroleum products [3–6]. This is ascribed to the fact that it can provide reproducible mass spectra with more structural information which allows library searching compared to soft ionization. Particularly when coupled to the high separation efficiency of gas chromatography (GC), it becomes a powerful tool for complex mixtures analysis [7–10], due to its high sensitivity and high information content, especially useful in the field of metabolomics [11–14]. On the other hand, the distribution of energy transferred during electron ionization results in a variety of products for a given analyte due to the large number of fragmentation pathways, which complicates the mass spectra.

However, it has been proposed by Mclafferty and Tureček [15] that preferred decomposition pathways are initiated at the favored radical and charge sites in the decomposing ion, and such a site was viewed as providing the driving force for specific types of reactions which are characteristic of the chemical nature of the site. For radical cations, cleavage reaction is induced either by positive charge site or by radical site, which corresponds to the heterolytic and homolytic cleavages, denoted as *i* and α, respectively [15].

In order to devise realistic mechanisms for how molecules fragment, the site of initial ionization must be defined at first [16], which is a key step for interpretation of EI mass spectra. The most favored radical and charge sites in the molecular ion are assumed to arise from the loss of the electron of lowest ionization energy (IE) in the molecule. Molecules with heteroatoms tend to ionize by loss of an electron from the *n*-orbitals of the heteroatoms, and

* Corresponding author.
E-mail address: yizeng_liang@263.net (Y.-Z. Liang).

1387-3806/$ – see front matter © 2009 Elsevier B.V. All rights reserved.
doi:10.1016/j.ijms.2009.07.004

compounds having double bonds or aromatic ring by loss of one of the π-electrons. Generally, the localization of most likely initial ionization site is determined by comparison with the approximate IEs of the functional groups in the molecule, based on the IEs of the most similar models [15]. Although it has proven to be very successful for aiding in EI mass spectral interpretation for most of molecules, there still remain some uncertainties some time, especially for the case that there are minor differences and nearly the equal values in the IE for comparable functional groups.

In the present, atomic spin density combined with molecular structures, was employed to investigation on the characteristic fragmentation patterns of the derivatives of tryptophan and tryptamine (shown in Fig. 1) by density functional theory (DFT) at the B3LYP/6–31+G (d, p) level. The main primary α-cleavage fragmentations induced by the radical site are defined through determining the localization of initial ionization site by natural spin density of molecular radical cations, in combination with the variations of the bond lengths from the ground state to cationic form.

There are three aspects which have to be addressed for choice of the derivatives of tryptophan and tryptamine. Firstly, identification of such indole alkaloids in mass spectrometry is very important for synthesis and characterization of natural products. Tryptophan is an essential amino acid for many organisms [17], and tryptamine and its derivatives are believed to play an important part as a neuromodulator or neurotransmitter, found in trace amounts in the brains of mammals [18]. Secondly, the primary α-cleavage fragmentation usually dominates the mass spectra for *N*-containing molecules, and the characteristic fragmentation patterns could be directly predicted from the produced base peak provided that the initial ionization site is determined by the spin density. Finally, the peak containing indole functional group usually dominates the spectra of such alkaloids due to the resonance-stabilized by the conjugation of the large aromatic ring, which is very useful for EI mass spectral interpretation of such alkaloids.

2. Experimental

The spectra for all the chosen molecules in this study are taken from the NIST (National Institute of Standards and Technology) Standard Reference Database of Mass Spectral Library (NIST05) (http://www.nist.gov/srd/index.htm), which are applied to further verify the reliability of the predicted results.

Optimization of geometries was preformed using Gaussian 03 program [19], employing the hybrid density functional theory (B3LYP) at the B3LYP/6–31+G (d, p) level. For the open-shell systems, unrestricted DFT method at the same level (UB3LYP/6–31+G (d, p)) was used. For computation of the spin densities, the atomic populations were obtained using natural population analysis (NPA) by the NBO 3.0 program incorporated into the Gaussian 03 package, based on the optimized structures at the UB3LYP/6–31+G (d, p) level. Spin contamination was minimal for all systems. Local minima and transition structures were optimized and verified by harmonic frequency analyses. Zero-point vibration energies were evaluated directly using the normal-mode frequencies without anharmonic scaling. Each transition structure was identified using the intrinsic reaction coordinates (IRC) method.

To assess the reliability of the present study for predicting characteristic fragmentation pathways, the initial ionization site predicted by this method was compared with those based on the approximate IEs of functional groups. The calculated spin densities for radical cations may be related to the questions of spin contamination. However, it has been demonstrated that hybrid functional B3LYP with 6–31+G (d, p) basis set is able to provide a good representation of the spin densities for doublet state, and moreover, it can be competitive with more expensive computational MP2 methods, without loss of the accuracy due to the inclusion of the electron-correlation [20,21]. To compare with the previous method for determination of the initial ionization site based on the IEs of similar models, the approximate IEs for the functional groups were obtained from Table 3.1 (page: 106) of reference [16].

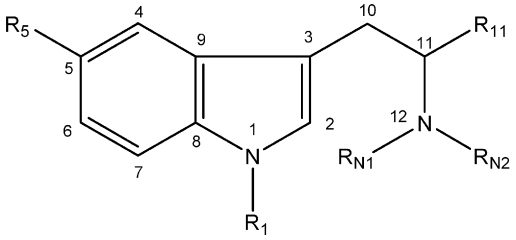

R_1=H	R_5=H	R_{11}= $COOCH_3$	R_{N1}=H	R_{N2}=H	**1**
R_1=H	R_5=H	R_{11}= COOH	R_{N1}=H	R_{N2}=CH_3	**2**
R_1=H	R_5=H	R_{11}= $COOCH_3$	R_{N1}=CH_3	R_{N2}=CH_3	**3**
R_1=CH_3	R_5= H	R_{11}= COOCH3	R_{N1}=CH3	R_{N2}=$COCH_3$	**4**
R_1=H	R_5=OH	R_{11}=H	R_{N1}=H	R_{N2}=H	**5**
R_1=H	R_5=CH_3	R_{11}=H	R_{N1}=H	R_{N2}=H	**6**
R_1=H	R_5=H	R_{11}=$COOC_2H_5$	R_{N1}=H	R_{N2}=H	**7**
R_1=H	R_5=H	R_{11}= COOH	R_{N1}= CHO	R_{N2}=H	**8**
R_1=H	R_5=H	R_{11}= COOH	R_{N1}=$COCH_3$	R_{N2}=H	**9**
R_1=H	R_5=H	R_{11}=COOH	R_{N1}=H	R_{N2}=COCH $(NH_2)CH_3$	**10**
R_1=H	R_5=OCH_3	R_{11}=H	R_{N1}=CH_3	R_{N2}=CH_3	**11**
R_1=H	R_5=H	R_{11}=H	R_{N1}=CH_3	R_{N2}=CH_3	**12**
R_1=H	R_5=OH	R_{11}=H	R_{N1}=CH_3	R_{N2}=CH_3	**13**

Fig. 1. General structure of the derivatives of tryptophan and tryptamine with different substituents.

3. Results and discussion

3.1. Spin densities

Atomic spin density, which reflects the unpaired electron density at a position of interest, usually at carbon in a radical, was applied to characterize the relative stability of the fragmentation radical through investigating on the electron delocalization [22–27]. In this work, atomic spin density, obtained by natural population analysis method at the unrestricted B3LYP/6–31+G (d, p) level of DFT theory, has been applied to determine on the localization of the radical site for molecular radical cations in order to predict the characteristic fragmentation pathways. This is ascribed to the fact that the radical site of radical cations can be regarded as the localization of the unpaired electron by redistribution after initial ionization, and thus can be reflected by the distribution of the spin density.

Since the most favorable fragmentation patterns for almost all the radical cations are induced by radical sites [15,16,28], determination of the radical site is very important for molecular radical cations to predict the preferred fragmentation pathways. Especially for molecules containing N atoms, the main primary α-cleavage fragmentation driven by radical becomes predominant and the produced base peak is usually 5–10 times more intense than any other peaks in the spectrum. The more intense base peak is the outstanding feature for such fragmentation, and thus the characteristic fragmentation pathways with respect to the main primary α-cleavage fragmentations could be defined if the radical site is determined by the spin density of molecular radical cations. As a comparison, the derivatives of tryptophan and tryptamine containing three different kinds of amine groups in aliphatic part are chosen for this research. The purpose of this choice is to test which kind of aliphatic amine groups can be comparable with the indole functional group for loss of an electron.

Table 1 lists the atomic spin densities, using NPA method at the B3LYP/6–31+G (d, p) level, of the molecular radical cations for L-tryptophan methyl ester (**1**), *N*-methyl tryptophan (**2**), *N*,*N*-dimethyltryptophan methyl ester (**3**), and L-tryptophan, *N*-acetyl-*N*, 1-dimethyl-, methyl ester (**4**), respectively, Also included are the corresponding expectation values of the S^2 operator. The $\langle S^2 \rangle$ for three molecular radical cations were determined to range from 0.7552 to 0.7605 compared to the expectation value of the $\langle S^2 \rangle$ with 0.75, indicating a good representation of the doublet state. It is worth noting that for the DFT method, the interpretation of $\langle S^2 \rangle$ is not straightforward because the DFT calculations yield electron densities, not electronic wave functions.

Table 1
UB3LYP/6–31G+ (d, p) computed spin densities of molecular radical cations and transition states of primary α-cleavage for **1**, **2**, **3** and **4**[a] in Fig. 1.

Atomic number	Natural spin densities						
	1•+	**TS1**	**2•+**	**TS21**	**3•+**	**TS31**	**4•+**
$\langle S^2 \rangle$[b]	0.7590	0.7580	0.7581	0.7573	0.7552	0.7577	0.7605
N_1	0.126	0.092	0.130	0.086	0.082	0.086	0.168
C_2	0.185	0.157	0.168	0.162	0.125	0.192	0.116
C_3	**0.314**	0.091	**0.287**	0.062	0.174	0.022	**0.357**
C_4	0.186	0.041	0.185	0.031	0.099	0.016	0.200
C_5	−0.049	−0.002	−0.044	0.001	−0.017	0.009	−0.050
C_6	0.137	0.023	0.127	0.016	0.062	0.005	0.139
C_7	0.047	0.016	0.061	0.014	0.036	0.018	0.059
C_8	0.026	−0.001	0.015	−0.002	0.006	−0.008	0.025
C_9	−0.061	−0.011	−0.055	−0.004	−0.032	0.006	−0.070
C_{10}	−0.006	0.082	−0.004	0.062	0.029	**0.215**	−0.012
C_{11}	0.027	**0.230**	0.028	0.184	0.011	**0.136**	0.027
N_{12}	0.019	**0.236**	0.061	**0.265**	**0.337**	**0.231**	0.004

The relatively larger values are marked in bold.
[a] L-Tryptophan methyl ester (**1**), *N*-methyltryptophan (**2**), *N*,*N*-dimethyltryptophan methyl ester (**3**), L-tryptophan, and *N*-acetyl-*N*, 1-dimethyl-, methyl ester (**4**).
[b] $\langle S^2 \rangle$ denotes the expectation value for different molecules.

From the spin density distribution, the main primary α-cleavage Fragmentation patterns induced by the radical site can be determined (shown in Schemes 1 and 2). It can be seen from Table 1 that for the radical cations **1•+**, **2•+**, and **4•+**, the spin densities mainly reside on the N_1, C_2, C_3, and C_4 atoms, and the largest spin density value of all atoms is for the C_3 atom, with 0.314, 0.287, and 0.357(see Table 1), respectively, implying that the initial ionization may occur preferentially on the N_1 atom followed by radical site rearrangement (see Scheme 1). As a result, the primary α-cleavage fragmentation is driven by the radical site occurring at C_3 atom, followed by homolytic cleavage of the C_{10}–C_{11} bond and the charge retention on the N_1 atom of indole functional group, which can be reflected by the changes of the spin density distribution from the reactions to transition states. This leads to loss of the aliphatic amine fragment and produces a base peak at *m*/*z* 130 or *m*/*z* 144 containing indole functional group, which is the outstanding feature for mass spectra of the alkaloids of tryptophan and tryptamine. However, the radical site for **3** is localized at N_{12} atom (with the largest spin density of 0.33) (see Table 1), and the primary α-cleavage fragmentation pattern is driven by the radical site at N_{12} atom. Although the breaking bond also involves between C_{10} and C_{11} atom, the charge ends up primarily with the N_{12} atom and the aliphatic amine part is included in the base peak *m*/*z* 116 due to the

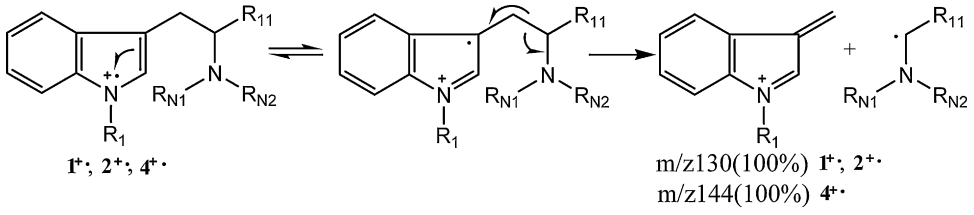

Scheme 1. Proposed main primary α-cleavage fragmentation pathways for radical cations of **1•+**, **2**·+, and 4·+.

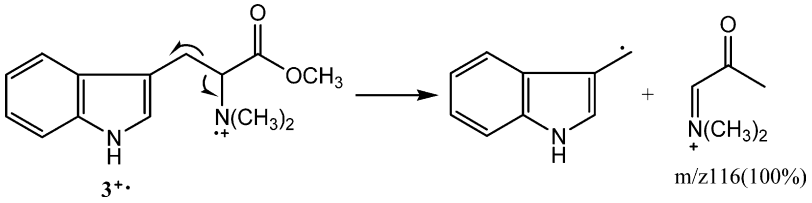

Scheme 2. Proposed main primary α-cleavage fragmentation pathway for radical cation **3•+**.

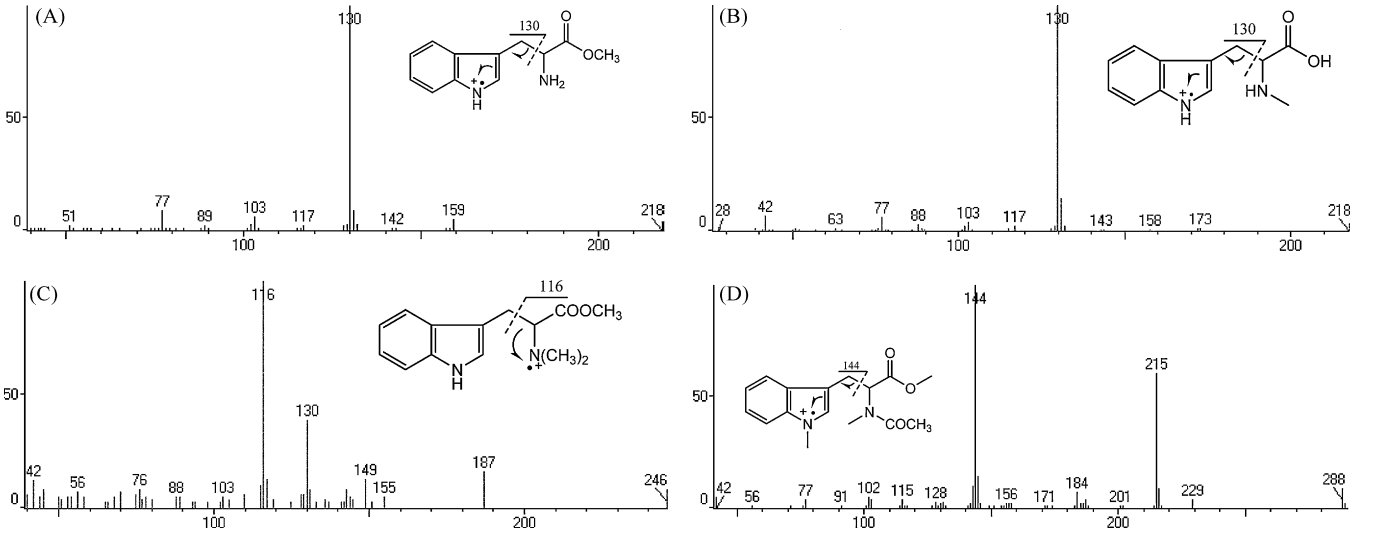

Fig. 2. Electron-impact mass spectra of the (A) **1**, tryptophan methyl ester (molecular weight: 218), (B) **2**, *N*-methyltryptophan (molecular weight: 218), and (C) **3**, *N*,*N*-dimethyltryptophan methyl ester (molecular weight: 246). (D) **4**, L-tryptophan, *N*-acetyl-*N*, 1-dimethyl-, methyl ester, respectively.

loss of the indole radical part. It is worth noting that the product ion containing the indole part also has relative more intense peak for **3** (*m*/*z* 130 is 39.3%), which is due to the resonance-stabilized by the conjugated effect of aromatic ring of the indole functional group. In addition, the relative smaller value of the largest spin density is mainly attributed to the delocalization of the unpaired electron over the ring after initial ionization.

The results show that the predicted primary α-cleavage fragmentation pathways for above four molecules are closely related to the base peak of the experimental mass spectra (shown in Fig. 2), indicating that using spin density to predict the radical-driven fragmentation patterns by determining the localization of the radical site is feasible. Therefore, the primary α-cleavage fragmentation of molecular radical cations can be defined as long as the localization of the radical site is determined by atomic spin density.

However, it is hardly assured whether the initial ionization site deduced from the determined radical site is correct, because the radical site of molecular radical cations represents the most likely localization of the unpaired electron by redistribution after initial ionization. Especially for the L-tryptophan, *N*-acetyl-*N*, 1-dimethyl-, methyl ester (**4**), it cannot confirmed whether the predicted result is correct evaluated just by spin density (listed in Table 1), because α-cleavage fragmentation of the C_{10}–C_{11} bond driven by the radical site produces equal *m*/*z* (144) ions wherever the initial ionization site occurs preferentially at either part of N atom. Thus, to further ensure the site of initial ionization, the variations of the molecular structures from neutral to cationic form must be considered.

3.2. Change in bond lengths

To aid in predicting preferred fragmentation pathway, variations in molecular structures from neutral molecules to molecular radical cations have been applied to determine the initial ionization site in this study.

Table 2 presents a part of bond lengths in the ground state and cationic form for **1**, **2**, **3**, and **4**, optimized at restricted and unrestricted B3LYP/6–31+G (d, p) method, respectively. Also included are the changes from the ground state to cationic form. It should be noted here that only the bonds with relative large changes are chosen. It is clear that there are large differences concerning the bonds of N_1–C_2 and C_2–C_3 for **1**, **2**, and **4**. The length of N_1–C_2 for both of them decreases greatly from the ground state to cationic form (0.047 Å, 0.044 Å, and 0.047 Å for **1**, **2** and **4**, respectively) and the increases for the C_2–C_3 bond arrive at significantly by 0.056 Å, 0.052 Å, and 0.054 Å for **1**, **2**, and **4**, respectively. In fact, these variations are attributed to the loss of the one of lone pair electrons for N_1 atom, leading to attraction of an electron from C_2–C_3 to pair up and thus shortening the bond of N_1–C_2. Meanwhile, the deficiency of the electron density results in the break of the double bond of C_2–C_3, with a significant lengthening of the C_2–C_3 bond. This further demonstrates that the most likely ionization site for **1**, **2** and **4** occurs at the N_1 atom, which is consistent with the predicted results by spin density. In contrast, the largest change of all bond lengths for **3** is related to that of C_{10}–C_{11} bond. The length of C_{10}–C_{11} for the molecular radical cation of **3** is about 0.043 Å much

Table 2
Comparison of the optimized bond lengths between the ground state and cationic radical form for **1**, **2**, **3**, and **4**, using UB3LYP/6–31G+ (d, p) level[a].

Bond	1	1•+	Δ1	2	2•+	Δ2	3	3•+	Δ3	4	4•+	Δ4
N_1–C_2	**1.382**	**1.335**	**−0.047**	**1.381**	**1.337**	**−0.044**	1.383	1.349	−0.034	**1.381**	**1.334**	**−0.047**
C_2–C_3	**1.376**	**1.432**	**0.056**	**1.376**	**1.428**	**0.052**	1.374	1.412	0.038	**1.377**	**1.431**	**0.054**
N_1–C_8	1.381	1.408	0.027	1.381	1.407	0.026	1.380	1.397	0.017	1.382	1.416	0.034
C_3–C_9	1.445	1.426	−0.019	1.445	1.427	−0.018	1.448	1.443	−0.005	1.442	1.426	−0.016
C_8–C_9	1.425	1.420	−0.005	1.422	1.419	−0.003	1.424	1.420	−0.004	1.423	1.419	−0.004
C_7–C_8	1.399	1.378	−0.021	1.401	1.379	−0.022	1.400	1.389	−0.011	1.401	1.379	−0.022
C_3–C_{10}	1.503	1.487	−0.016	1.503	1.487	−0.016	1.505	1.482	−0.023	1.500	1.489	−0.011
C_{10}–C_{11}	1.562	1.568	0.006	1.561	1.574	0.013	**1.568**	**1.611**	**0.043**	1.570	1.580	0.01
C_{11}–N_{12}	1.456	1.461	0.005	1.447	1.446	−0.001	1.455	1.427	−0.028	1.448	1.445	−0.003

The bold values are referred to the significantly changes of bond lengths from ground state to cationic form.

[a] **1**•+, **2**•+, **3**•+, and **4**•+ denote the molecular radical cations corresponding to the ground state, respectively. Δ1, Δ2, Δ3, and Δ4 represent the variations from the ground state to cationic form, respectively.

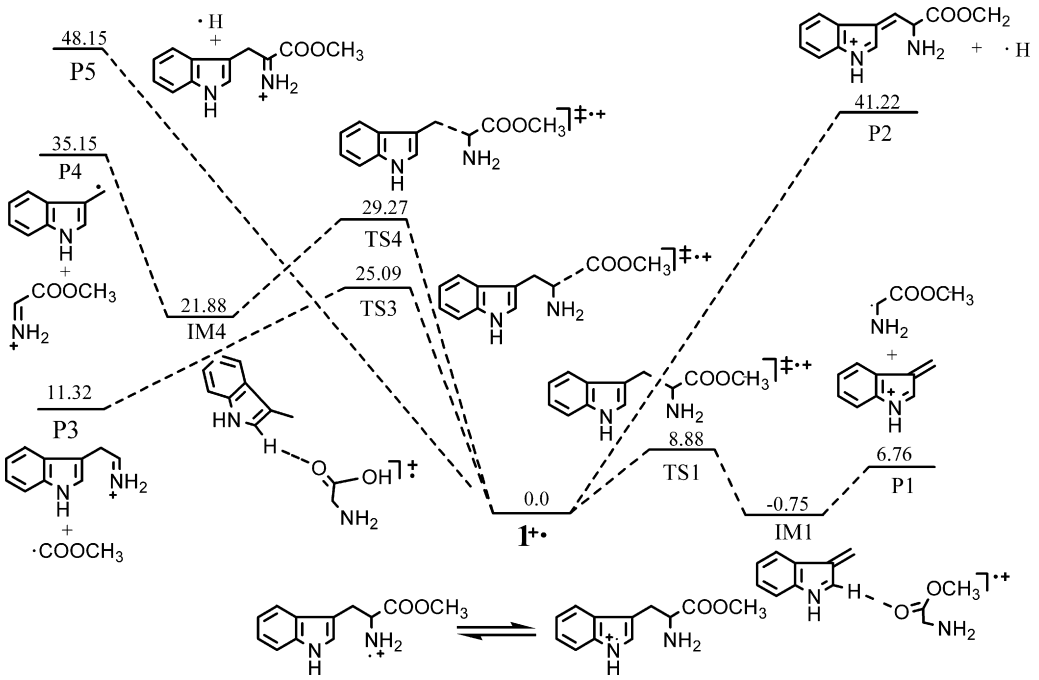

Fig. 3. Gibbs energy profiles at 298 K for all possible α-cleavage fragmentation pathways of radical cation **1**•+ at UB3LYP/6–31G+ (d, p) level. All numbers (in kcal/mol) are relative to **1**•+.

longer that that in ground state. So it can be deduced that the initial ionization site for **3** occurs preferentially at N_{12}, thus inducing the α-cleavage of C_{10}–C_{11} by the radical site with charge retention in tertiary aliphatic amine fragment.

The results indicate that the variations of the bond from neutral to cationic form are helpful for predicting the primary α-cleavage fragmentation patterns. In combination with the change of the bond lengths from neutral to cationic molecule, the initial ionization site can be deduced by the determined radical site. Particularly for the molecule of **4**, the initial ionization site can be further confirmed through analyzing the significant changes of the related bonds. A significant contraction of the N_1–C_2 bond (1.381–1.334 Å) and expansion of the C_2–C_3 bond (1.377–1.431 Å) from ground state to radical cation indicate that easily loss of an electron occurs at the N_1 atom of indole functional group. Thus, the main primary α-cleavage fragmentation can be proposed in Scheme 1 and the base peak at *m*/*z* 144 should correspond to the indole functional group, which is well consistent with the experimental mass spectrum listed in Fig. 2d.

Thus, the main primary α-cleavage fragmentation can be predicted through determining the site of initial ionization by the combination of the spin density and change of the molecular structures, which can be considered as the specific fragmentation patterns for characterizing such simple indole alkaloids.

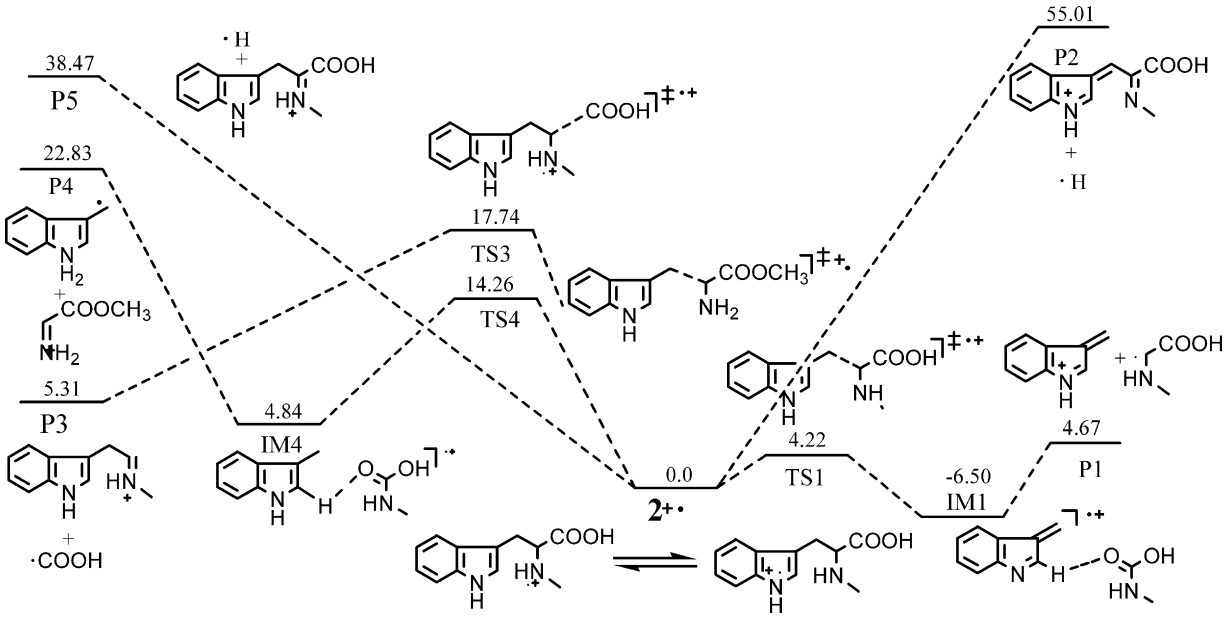

Fig. 4. Gibbs energy profiles at 298 K for all possible α-cleavage fragmentation pathways of radical cation **2**•+ at UB3LYP/6–31G+ (d, p) level. All numbers (in kcal/mol) are relative to **2**•+.

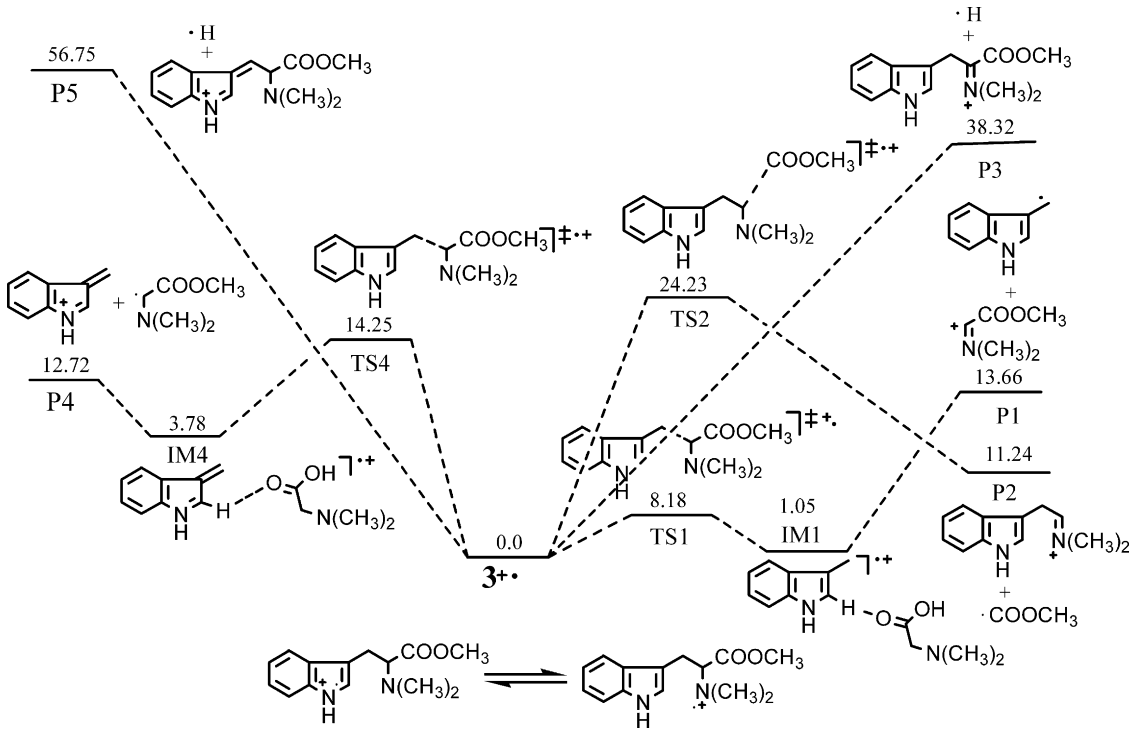

Fig. 5. Gibbs energy profiles at 298 K for all possible α-cleavage fragmentation pathways of radical cation **3**•+ at UB3LYP/6–31G+ (d, p) level. All numbers (in kcal/mol) are relative to **3**•+.

3.3. α-Cleavage fragmentation pathways of radical cations 1•+, 2•+, and 3•+

In addition to the absolute predominance of primary α-cleavage dissociation related to the base peak, there also exist some other competitive α-cleavage fragmentations induced by radical site. To better understand the mechanisms of fragmentation processes and further confirm the reliability of the predicted results obtained by spin density and computed geometries discussed above. Figs. 3–5 show all five possible α-cleavage fragmentations of radical cations **1**•+, **2**•+, and **3**•+, respectively, ionized at N atom either in indole or in aliphatic amine group.

As can be seen in Fig. 3, when ionization occurs initially at N_3 atom contained in indole part (right side of Fig. 3), **1**•+ can lose either of glycine methyl ester part to prominently produce *m*/*z* 130 peak or H• radical associated with C_{12} atom to give the ion having *m*/*z* 217. For the case that initial ionization site is located at amine N_{12} atom, there are three possible α-cleavage fragmentation pathways (left side of Fig. 3): (a) loss of •$COOCH_3$ radical leads to the *m*/*z* 159 ion peak (5.2%) via the transition state TS3, or (b) dissociation of the C_{10}–C_{11} bond produces the ion having *m*/*z* 88 (1.2%) through the IM4 after across the TS4, or (c) loss of the H• radical from the C_{11} atom gives the *m*/*z* 217 peak. Actually, the *m*/*z* 217 ion peak is not found in mass spectrum and thus these two reactions involving H• radical loss for above two cases do not occur, due to the relatively high Gibbs free energies (ΔG^0_{298} = 41.22 kcal/mol and 48.15 kcal/mol). In general, cleavage of the C_{10}–C_{11} bond can result in two different reactions(**1**•+ → TS1 → IM1 → P1) and (**1**•+ → TS4 → IM4 → P4). The competition between these two channels depends largely on the ionization energy of the fragment. Moreover, the energy barrier of TS1 (ΔG^0_{298} = 8.8) is also much lower than that of TS4 (ΔG^0_{298} = 29.27), indicating that the more favorable process corresponds to the loss of the $NH_2CH{\cdot}COOCH_3$ radical with charge retention on the indole system. Obviously, this reaction is also the most favored fragmentation pathway among the five α-cleavage dissociations. In addition, the relative lower free energy of intermediate IM1 is mainly attributed to the strong hydrogen bond from H atom in indole ring to O atom of carbonyl group, in which the distance is only 2.051 Å. It should be noted that a potential energy scan increasing the C–H bond distance in **1**•+ results in a monotonic increase in energy and energy barrier against the fragmentation is thus determined by its reaction energy.

It can be seen more clearly in Fig. 4 that dissociation of ion **2**•+ almost has the same α-cleavage fragmentation patterns as those of **1**•+. The most preferred fragmentation among all the five α-cleavage dissociations also involves the C_{10}–C_{11} bond cleavage after initial ionized at N_3 atom by loss of carbonyl-contained group, giving the base peak at *m*/*z* 130. Furthermore, the Gibbs energy of TS1 (ΔG^0_{298} = 4.22 kcal/mol) against the conversion of **2**•+ into intermediate IM1 is even lower than that of corresponding **1**•+ (ΔG^0_{298} = 8.88 kcal/mol) (right side of Fig. 4). On the contrary, for the dissociation of the ion **3**•+, the most energetically favored fragmentation corresponds to the loss of indole-containing radical to produce 116 *m*/*z* base peak after C_{10}–C_{11} cleavage, initially ionized at N_{12} atom in aliphatic part (right side of Fig. 5).

In addition, for radical cations **1**•+ and **2**•+, the spin densities originally residing on the C_3 atom have transferred into the C_{11} and C_{12} atoms from radical cations to transition states (see Table 1), indicating that the C_{10}–C_{11} bond cleavage involves loss of aliphatic part and the charge remains in the indole system. Whereas for the **3**•+ the spin density mainly located at N_{12} atom has transferred into the C_{10} and C_{11} atoms from the reaction to TS31, implying that dissociation of C_{10}–C_{11} bond involves loss of indole system with charge retention on the aliphatic group after initially ionized at N_{12} atom.

3.4. Compared with ionization energy for determination of initial ionization site

Determining the initial ionization site is a key step for predicting the preferred fragmentation pathways so as to unravel the mechanisms of the fragmentation reaction in detail, which must

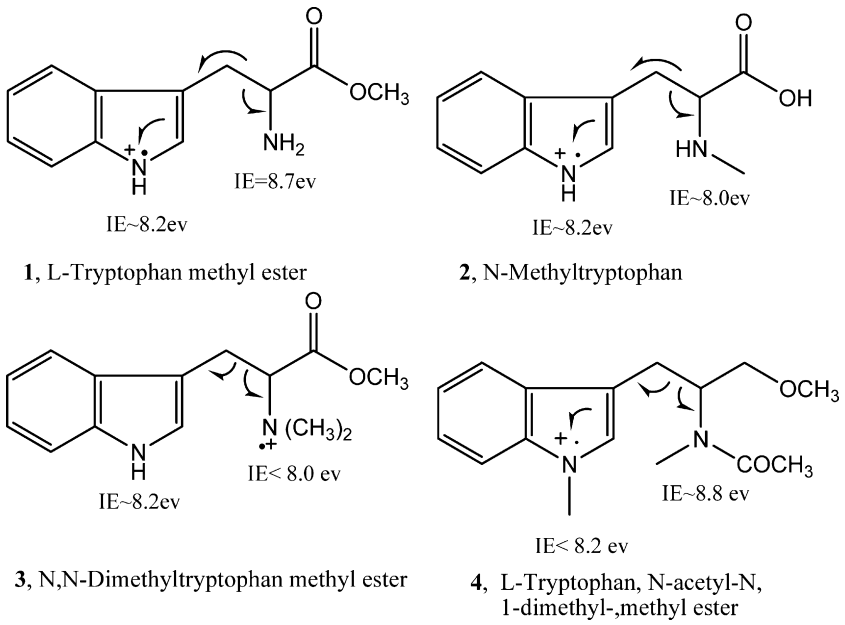

Fig. 6. The most likely initial ionization sites are defined based on the ionization energies of functional groups.

be defined at first in the mass spectra interpretation not only for small molecules [15,16], but also for gas-phase peptides [28–32]. In general, the most favorable initial ionization site could be evaluated by comparison with the approximate IEs for the functional groups in the molecule, based on the IEs of appropriate model compounds [15,16]. However, the discussion above displays that the initial ionization site can also be defined using spin density distributions and the change of the bond lengths. To test the reliability of this method, the molecules of **1**, **2**, **3**, and **4** are chosen for comparison with IE for determination of initial ionization site in this research.

Fig. 6 shows the most likely initial ionization sites for the chosen molecules of **1**, **2**, **3**, and **4** defined based on the IEs of functional groups. It can be seen, for the analyte of **1**, that the initial ionization will occur primarily on the N atom contained in indole functional group because the IE (IE ~8.2 eV) for loss of an electron from the N atom in the indole functional group is lower than that from the N atom contained in amine group (IE ~8.7 eV). Similarly, the initial ionization site for **2** and **4** is also located at N atom of indole functional group, according to the IEs of comparable functional groups, whereas it occurs at N atom of the aliphatic amine group for **3**. As a result, the predicted results of **1**, **3**, and **4** are consistent with the experimental mass spectra, as well as those by the DFT method in this study, while for **2** the result is just contrary to the present result and experimental mass spectrum. Based on the comparable IEs between indole system (8.2 eV) and secondary amine group (8.0 eV), the N atom in secondary amine part should be the favorable initial ionization site. However, the spectrum for **2** in Fig. 2(B) shows that product ion at *m*/*z* 130 becomes predominant, indicating that the localization of the initial ionization site is actually located at N atom in indole group, although there is a little difference in IE between them.

The inaccuracy of the predicted result of **2** based on the IE is mainly attributed to the small differences in IE between two groups, making it hardly determine the primary ionization site. However, according to the view of the point, the N atom in the two functional groups should have nearly the same probability for primary loss of the electron, but actually the produced base peak having *m*/*z* 130 corresponding to the initial ionization site at N_1 is more intense than that of *m*/*z* 116 with initial ionization site at N_{12} for the mass spectrum of **2** (see Fig. 2(B)). This indicates that the abundances of the produced ions in mass spectrum strongly depend on the localization of the ini-

Table 3
UB3LYP/6–31G+ (d, p) computed spin densities for the molecular cationic radicals of the derivatives of tryptophan and typtamine for Fig. 1[a].

Atomic number	Natural spin densities								
	5•+	**6**•+	**7**•+	**8**•+	**9**•+	**10**•+	**11**•+	**12**•+	**13**•+
$\langle S^2 \rangle$	0.7558	0.7569	0.7552	0.7613	0.7615	0.7602	0.7510	0.7558	0.7553
N_1	0.118	0.142	0.172	0.128	0.155	0.138	0.143	0.099	0.102
C_2	0.176	0.145	0.118	0.175	0.148	0.166	0.018	0.121	0.067
C_3	**0.239**	**0.252**	**0.276**	**0.312**	**0.309**	**0.289**	0.165	0.147	0.175
C_4	0.187	0.176	0.215	0.224	0.214	0.237	0.154	0.092	0.117
C_5	−0.037	−0.023	−0.017	−0.064	−0.040	−0.051	0.042	−0.014	0.003
C_6	0.122	0.081	0.105	0.167	0.132	0.148	−0.024	0.056	0.012
C_7	0.074	0.065	0.135	0.063	0.099	0.095	0.072	0.039	0.036
C_8	0.012	−0.002	−0.020	0.024	0.001	0.007	−0.025	0.001	−0.012
C_9	−0.047	−0.049	−0.053	−0.058	−0.059	−0.052	−0.024	−0.029	−0.025
C_{10}	0.005	0.020	−0.006	−0.009	0.007	−0.008	0.038	0.047	0.040
C_{11}	0.028	0.034	0.027	0.025	−0.001	0.023	0.011	0.011	0.010
N_{12}	0.105	0.167	0.030	0.003	0.027	0.006	**0.327**	**0.376**	**0.381**

The bold values are referred to the relatively large spin densities.

[a] **5**, **6**, **7**, **8**, **9**, **10**, **11**, and **12** denote the compounds of 5-hydroxytryptamine, methyltryptamine, tryptophan ethyl ester, *N*-formyltryptophan, D,L-acetyltryptophan, L-alanyl-L-tryptophan, 5-methoxydimethyltryptamine, dimethyltryptamine, and 5-hydroxy-*N*,*N*-dimethyltryptamine, respectively.

Table 4
Comparison of the changes of bond lengths from ground state to cationic form for compounds of **5**, **6**, **7**, **8**, **9**, **10**, **11**, **12**, and **13** at UB3LYP/6–31+G(d, p) level.

Bond	5	6	7	8	9	10	11	12	13
N_1–C_2	**−0.043**	**−0.045**	**−0.056**	**−0.046**	**−0.05**	**−0.052**	−0.021	−0.031	0.012
C_2–C_3	**0.058**	**0.053**	**0.067**	**0.056**	**0.06**	**0.063**	0.022	0.033	0.027
N_1–C_8	0.023	0.025	0.024	0.026	0.026	0.022	0.001	0.012	−0.030
C_3–C_9	−0.022	−0.013	−0.025	−0.024	−0.026	−0.016	0.015	−0.011	−0.004
C_8–C_9	−0.019	−0.018	−0.018	−0.001	−0.001	−0.014	−0.013	−0.005	−0.014
C_7–C_8	−0.026	−0.026	−0.026	−0.022	−0.033	−0.023	0.012	−0.012	−0.004
C_3–C_{10}	−0.022	−0.033	−0.024	−0.011	−0.014	−0.018	−0.031	−0.029	−0.025
C_{10}–C_{11}	0.033	0.04	0.013	0.014	0.025	0.014	**0.063**	**0.074**	**0.072**
C_{11}–N_{12}	−0.024	−0.031	0.012	−0.003	0.001	0.002	**−0.041**	**0.033**	**0.042**

The relatively significant changes are marked in bold.

tial ionization site, and have significantly differences for the case of even minor differences in the IE between the two comparable functional groups in molecules. Thus, it further demonstrated the importance of accurately determining initial ionization site for understanding the mass spectra. On the other hand, the ambiguous IE used for the comparison functional groups is another reason for hardly ensuring the initial ionization site. Because the IEs of the functional groups in the molecule are estimated based on the approximate IEs of the appropriate models, it is inaccuracy when the surrounding environments are changed. Moreover, to the best of our knowledge, there is no method which can provide the exact IE values for radicals and molecules until now.

However, the spin density of molecular radical cation exactly determines the localization of the radical-initiation site quantitively. In combination with the change of the related bonds, the localization of the initial ionization site can be confirmed. As compared to those based on the IE, it provides a new approach for determining the initial ionization site, and can produce more accurate predicted results for determining the preferred fragmentation in the EI mass spectra, which will play an important part in predicting the mechanisms of the fragmentation patterns.

It should be noted that this study focuses only on the α-cleavage fragmentation induced by radical site for molecules containing electron donors such as N, O, S, π-bond. Because, in those cases where charge-directed pathways are minimized, the radical-induced α-cleavage dominates the primary fragmentation, the primary α-cleavage fragmentation can be easily obtained through determining the localization of initial ionization site for molecular radical cations by spin density and change of the bond lengths, which is the characteristic fragmentation patterns for such kinds of molecules. However, not all radical cations fragment via radical-induced process. For other cases that there is a competition between the radical-site and charge-site induced reactions and the charge and radical are located on the same atom, it still remains some uncertainties to determine which kind of the induced reaction dominates the fragmentation, even although the initial ionization site has been determined. However, combined with the experimental mass spectra, most of charge-site-initiated reactions can also be predicted if the initial ionization site has been determined by combination the spin density and geometry changes of the molecules.

3.5. Application

In the section above, the DFT method performs well in predicting the favorable α-cleavage fragmentation mechanisms for **1**, **2**, **3** and **4**, which is even prior to those by the IE method. However, to further assess the applicability of the method, several derivatives of tryptophan and tryptamine, which include three different types of amine groups in aliphatic part, are chosen. The first three molecules include 5-hydroxytryptamine (**5**), methyltryptamine (**6**), and tryptophan ethyl ester (**7**), in which the primary amines are contained in the aliphatic parts. The second type is referred to the molecules in which the aliphatic amine groups belong to the secondary amines, containing *N*-formyltryptophan (**8**), D,L-acetyltryptophan (**9**), and L-alanyl-L-tryptophan (**10**). The last case is that the aliphatic parts are the tertiary amines, containing 5-methoxydimethyl tryptamine (**11**), dimethyltryptamine (**12**), and 5-hydroxy-*N*, *N*-dimethyltryptamine (**13**).

For these molecules, the characteristic fragmentation patterns corresponding to the main primary α-cleavage could easily be predicted, as long as the atomic spin density of the molecular radical cations and the variations of bond lengths from neutral to cationic molecules are obtained. This is because that the main primary α-cleavage fragmentation induced by the radical site dominates the mass spectra and produces significant base peak, as compared to other produced ions. In addition, there are competitive α-cleavage fragmentations induced by the radical site between the indole functional group and aliphatic amine group, the main fragmentation pathway depended on which *N*-containing part the initial ionization site is located. As a result, the base peak produced by the primary α-cleavage fragmentations can be regarded as the specific mass spectra for characterizing such simple indole alkaloids.

Table 3 lists the values of natural spin density at the UB3LYP/6–31G+(d, p) level and the corresponding expectation values of the S^2 operator. It can be seen that the largest $\langle S^2 \rangle$ is smaller than 0.7613, indicating the better performances of the DFT theory for these unrestricted systems. The largest spin density resides on the C_3 atom for the first two types of molecules (**5**, **6**, **7**, **8**, **9**, and **10**), whereas it is located on the N_{12} atom for the last kinds of compounds (**11**, **12**, and **13**). This indicates that the α-cleavage of C_{10}–C_{11} bond for the first two types of molecules is induced by the radical site on the C_3 atom, with charge retention in the indole part, while the α-cleavage fragmentation for the last kinds of compounds is driven by the radical site on the N_{12} atom, with charge retention in the tertiary amines. With the changes of the bond lengths from the neutral to cationic molecules listed in Table 4, it can be further assured that initial ionization must occur at N_1 and N_{12} atom for such two situations, respectively. It can be seen that the significant changes of the bonds are mainly focused on the bonds of N_1–C_2 and C_2–C_3 for the first two kinds of six molecules, while it is related to the C_{10}–C_{11} and C_{11}–N_{12} bond for the last three molecules. For the neutral state of the six molecules, a significant shortening of the N_1–C_2 and lengthening of the C_2–C_3 bond compared to their cationic forms, indicate that the ionization is predicted to occur primarily on the N_1 atom, because the lack of an electron for N_1 atom will make it attract electron density from the bond of C_2–C_3 to form the double bond with the left electron of lone pair, shortening the N_1–C_2 greatly and simultaneously lengthening the bond of C_2–C_3 significantly due to the cleavage of the π bond between C_2 and C_3 atoms. For the last three molecules, on the other hand, the largest expansion is related to the C_{10}–C_{11} bond, which increases nearly by an average of 0.07 Å upon removing an electron from neutral to radical cationic molecule. This implies that the most likely

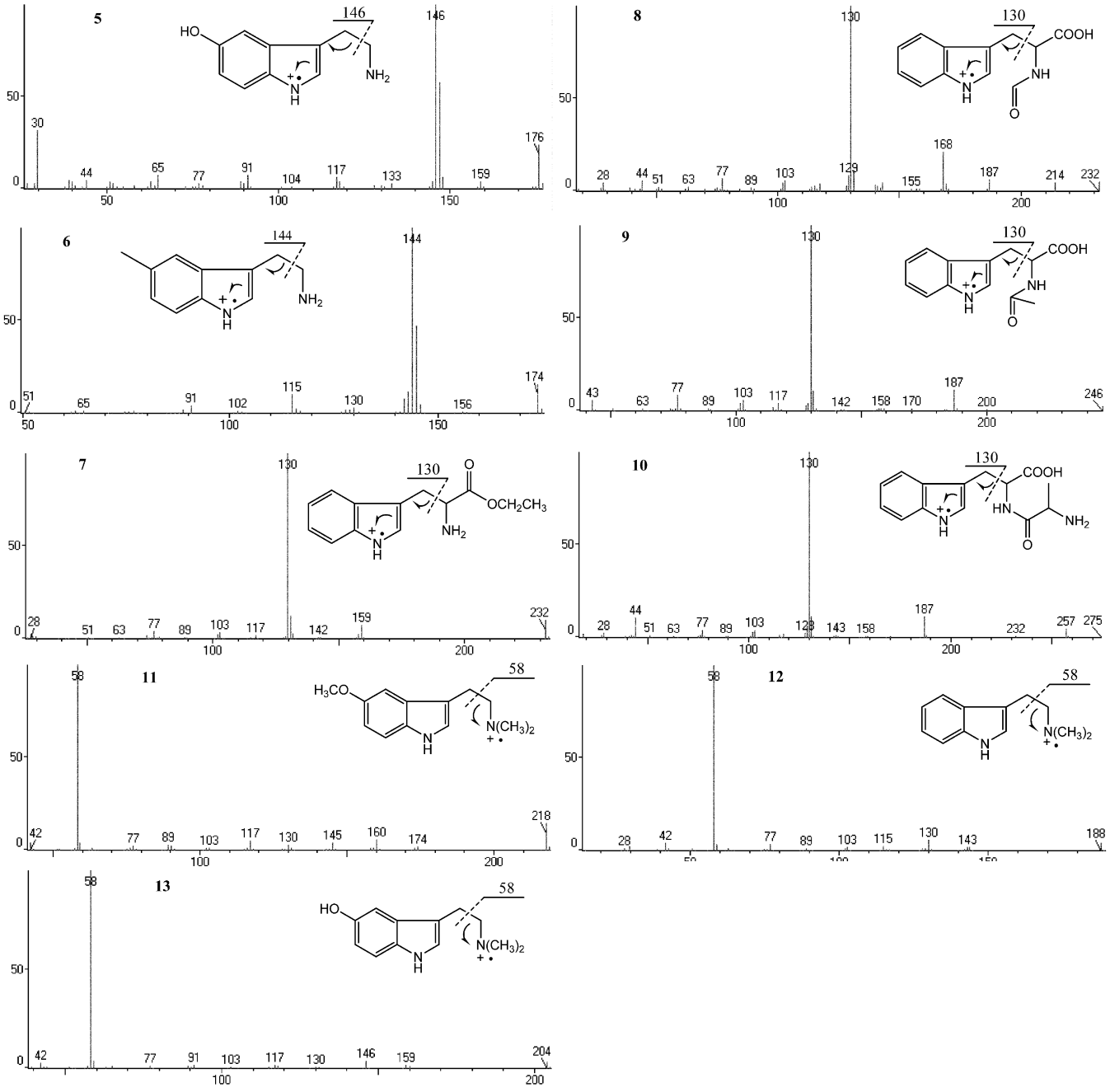

Fig. 7. Electron-impact mass spectra for the compounds of **5**, **6**, **7**, **8**, **9**, **10**, **11**, **12**, and **13**, respectively.

localization of the initial ionization sit is at the N_{12} atom, and the charge and radical are both located at N_{12} atom. The trend for the changes of the bond for two such cases agrees well with the spin density distributions.

Fig. 7 gives the mass spectra of the three kinds of chosen molecules mentioned above. Also included are the initial ionization site defined in this work. The characteristic fragmentations patterns predicted in the present method are in good agreement with the experimental mass spectra. The more intense base peak closely related to the main primary α-cleavage fragmentation of molecular radical cation can be determined by the initial ionization site. The results also show that for the simple indole alkaloids such as tryptophan, tryptamine, and its derivatives, loss of an electron easily occurs at the N_1 atom in the indole functional groups for the primary and secondary amines containing in the aliphatic part, but the preferred ionization occurs at the N_{12} atom for the case of the tertiary amine groups included in the aliphatic part. Therefore, the present method can be applied to predict the preferred fragmentation pathways for radical-driven dominated fragmentation.

4. Conclusion

A novel method for determining the most likely initial ionization site by the natural spin density and molecular structures using the DFT theory at B3LYP/6–31+G (d, p) level, has been proposed in this study. To test the reliability and accuracy of the present study, the main primary α-cleavage fragmentations for the derivatives of trytophan and tryptamine are evaluated through determining the initial ionization site of molecular radical cation by spin density and the change of bond lengths from neutral to cationic molecules,

and the produced more intense base peak can be viewed as the characteristic fragmentation mechanisms for EI mass spectra interpretation of such simple indole alkaloids. Furthermore, the results have been compared with the experimental mass spectra and those by the IE method. The results show that the characteristic fragmentation mechanisms predicted in the present method agree well with those of experimental mass spectra, and can be comparable to those by the IE method. It will play an important role in the EI mass spectra interpretation of such simple indole alkaloids of the derivatives of tryptophan and tryptamine.

However, some limitations related to this study should be addressed. First, this study is unsuitable for negative ions. Second, it still remains some uncertainties for the cases that there is the competition between the radical-site-initiated and charge-site-initiated reactions when the charge and radical kept at the same atom, because it cannot be assured which kind of the induced model dominates even though the initial ionization site has been confirmed.

Notwithstanding its limitation, determining the initial ionization site by the spin density and molecular structures is very useful for interpretation of mass spectra of molecules in which the α cleavage becomes predominant, especially important for the *N*-containing molecules. Moreover, it can be also used to understand radical-driven fragmentation mechanisms for gas-phase peptide occurring in electron capture dissociation (ECD) [28], electron transfer dissociation (ETD) [29], or low-energy CID of peptide radical cations [31,32].

Acknowledgements

This work is financially supported by the National Nature Foundation Committee of PR China (grants no. 20875104), the international cooperation project on traditional Chinese medicines of ministry of science and technology of China (grant nos. 2006DFA41090 and 2007DFA40680). The studies meet with the approval of the university's review board.

References

[1] R. Aebersold, D.R. Goodlett, Chem. Rev. 101 (2001) 269.
[2] X. Zhang, D. Wei, Y. Yap, L. Li, S. Guo, F. Chen, Mass Spectrom. Rev. 26 (2007) 403.
[3] K. Dettermer, P.A. Aronov, B.D. Hammock, Mass Spectrom. Rev. 26 (2007) 51.
[4] Y.Z. Liang, P. Xie, K. Chan, J. Chromatogr. B 812 (2004) 53.
[5] M. Thevis, W. Shanzer, Mass Spectrom. Rev. 26 (2007) 79.
[6] C.E. Wheelock, M.E. Colvin, J.R. Sanborn, B.D. Hammock, J. Mass Spectrom. 43 (2008) 1053.
[7] F. Gong, Y.Z. Liang, Q.S. Xu, F.T. Chau, J. Chromatogr. A 905 (2001) 193.
[8] F. Gong, Y.Z. Liang, H. Cui, F.T. Chau, B.T.P. Chan, J. Chromatogr. A 909 (2001) 237.
[9] P. Jonsson, A.I. Johansson, J. Gullberg, J. Trygg, J.A.B. Grung, S. Marklund, M. Sjstrm, H. Antti, T. Moritz, Anal. Chem. 77 (2005) 5635.
[10] H. Kanai, P.K. Chrysanthopoulos, M.I. Klapa, J. Chromatogr. B 871 (2008) 191.
[11] T. Kuhara, Mass Spectrom. Rev. 24 (2005) 814.
[12] S.G.V. Bôas, D.G. Delicado, M. Akesson, J. Nielsen, Anal. Biochem. 322 (2003) 134.
[13] T. Kuhara, J. Chromatogr. B 781 (2002) 497.
[14] C. Wittmann, M. Hans, E. Heinzle, Anal. Biochem. 307 (2002) 379.
[15] F.W. Mclafferty, F. Tureček, Interpretation of Mass Spectra, University Science Books, Sausalito, 1993.
[16] R.M. Smith, Understanding Mass Spectra: A Basic Approach, second edition, John Wiley & Sons, Inc., Hoboken, New Jersey, 2004.
[17] E.M. Adkins, E.L. Barker, R.D. Blakerly, Mol. Pharmacol. 59 (2001) 514.
[18] S. Hibino, T. Choshi, Nat. Prod. Rep. 18 (2001) 66.
[19] M.J. Frisch, G.W. Trucks, H.B. Schlegel, G.E. Scuseria, M.A. Robb, J.R. Cheeseman, J.A. Montgomery Jr., T. Vreven, K.N. Kudin, J.C. Burant, J.M. Millam, S.S. Iyengar, J. Tomasi, V. Barone, B. Mennucci, M. Cossi, G. Scalmani, N. Rega, G.A. Petersson, H. Nakatsuji, M. Hada, M. Ehara, K. Toyota, R. Fukuda, J. Hasegawa, M. Ishida, T. Nakajima, Y. Honda, O. Kitao, H. Nakai, M. Klene, X. Li, J.E. Knox, H.P. Hratchian, J.B. Cross, V. Bakken, C. Adamo, J. Jaramillo, R. Gomperts, R.E. Stratmann, O. Yazyev, A.J. Austin, R. Cammi, C. Pomelli, J.W. Ochterski, P.Y. Ayala, K. Morokuma, G.A. Voth, P. Salvador, J.J. Dannenberg, V.G. Zakrzewski, S. Dapprich, A.D. Daniels, M.C. Strain, O. Farkas, D.K. Malick, A.D. Rabuck, K. Raghavachari, J.B. Foresman, J.V. Ortiz, Q. Cui, A.G. Baboul, S. Clifford, J. Cioslowski, B.B. Stefanov, G. Liu, A. Liashenko, P. Piskorz, I. Komaromi, R.L. Martin, D.J. Fox, T. Keith, M.A. Al-Laham, C.Y. Peng, A. Nanayakkara, M. Challacombe, P.M.W. Gill, B. Johnson, W. Chen, M.W. Wong, C. Gonzalez, J.A. Pople, Gaussian 03, Revision E. 01, Gaussian, Inc., Wallingford, CT, 2004.
[20] G.M. Jensen, D.B. Goodin, S.W. Bunte, J. Phys. Chem. A 100 (1996) 954.
[21] F. Himo, L.A. Eriksson, J. Phys. Chem. B 101 (1997) 9811.
[22] J.B. Gilroy, S.D. Mckinnon, P. Kennepohl, M.S. Zsombor, M.J. Ferguson, L.K. Thompson, R.G. Hicks, J. Org. Chem. 72 (2007) 8062.
[23] M. Pesola, J.V. Boehm, S. Pőykkő, R.M. Nieminen, Phys. Rev. B 58 (1998) 1106.
[24] F.D. Vleeschouwer, V.V. Speybroeck, M. Waroquier, P. Geerlings, F.D. Proft, J. Org. Chem. 73 (2008) 9109.
[25] S.E. Walden, R.A. Wheeler, J. Phys. Chem. 100 (1996) 1530.
[26] N. Claiser, M. Souhassou, C. Lecomte, B. Gillon, C. Carbonera, A. Caneschi, A. Dei, D. Gatteschi, A. Bencini, Y. Pontillon, E.L. Berna, J. Phys. Chem. B 109 (2005) 2723.
[27] H.W. Zhou, N.B. Wong, K.C. Lau, A. Tian, W.K. Li, J. Phys. Chem. A 111 (2007) 9838.
[28] C.K. Barlow, R.A.J. O'Hair, J. Mass Spectrom. 43 (2008) 1301.
[29] M. Sobczyk, D. Neff, J. Simons, Int. J. Mass Spectrom. 269 (2008) 149.
[30] J. Laskin, J.H. Futrell, I.K. Chu, J. Am. Chem. Soc. 129 (2007) 9598.
[31] I.K. Chu, J.F. Zhao, M. Xu, S.O. Siu, A.C. Hopkinson, K.W.M. Siu, J. Am. Chem. Soc. 130 (2008) 7862.
[32] S. Wee, R.A.J. O'Hair, W.D. Mcfadyen, Int. J. Mass Spectrom. 234 (2004) 101.